CHAPTER FIVE : OISF LENGTH, WIDTH AND DEPTH

5.1 Objective and Experimental

After the basic information about preferential etching is gathered, OISF dimension change as a function of depth was looked into, to determine the impact of excessive etching to OISF dimension. Measurement of OISF length and width on the same piece of (100) and (111) wafer, intermittent with repeated etching, using Atomic Force Microscope (AFM) was carried out.

However there are limitations in OISF depth measurement by AFM. Depth measurement by AFM is limited by the shape and size of AFM silicon probe tip used. For any valley opening of less than 5μm, AFM cannot measures its depth accurately. Preliminary study showed than OISF width is less than 5μm therefore an alternative OISF depth measurement method was used. (*Refer Appendix A: limitation of depth measurement using AFM*).

Polished wafers with crystal orientation (100) and (111) were sand blasted then oxidized in oxygen for an hour at 1100°C using heat cycle showed in Figure 5.1. OISFs were formed on the sand blasted region during oxidation and oxide formed was stripped off with hydrofluoric acid (HF). A cross, "+", was marked on sand blasted surface with a diamond pen as reference point so that we could return to the same piece of OISF to study OISF length and width change (*Refer Figure 5.2*).

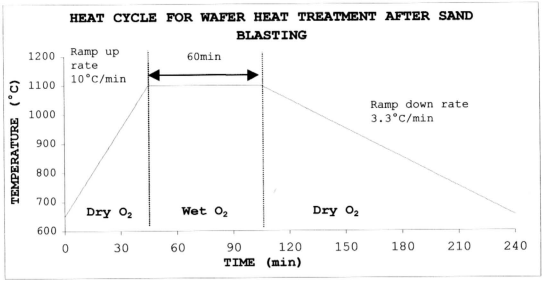

Figure 5.1 : Heat cycle for wafer heat treatment after sand blasting.

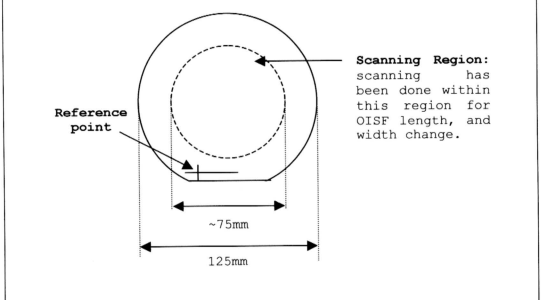

Figure 5.2 : Reference point is marked on wafer surface for repeated scanning of the same area on wafer surface.

Preferentially etched (100) and (111) wafers (20s etched) were scanned at one spot with scanning area of 40μm x 40μm, using AFM at setting showed in Table 3.3. Further scanning of same spot was carried out after every etching until 220s

etching time was reached. Surface removal by etching process was determined from etching rate obtained experimentally.

OISF length and width were measured from AFM scanned images. Figure 5.3 is a typical cross sectional diagram of OISF along its longer axis. The OISF length is labeled as L in Figure 5.3. OISF length is the horizontal distance between the red markers. Figure 5.4 is the cross sectional view of OISF along its shorter axis at the middle point of its length. OISF width is labeled as W in Figure 5.4 and is the horizontal distance between the two red markers. The same measurement was repeated at different surface removal by repeated etching.

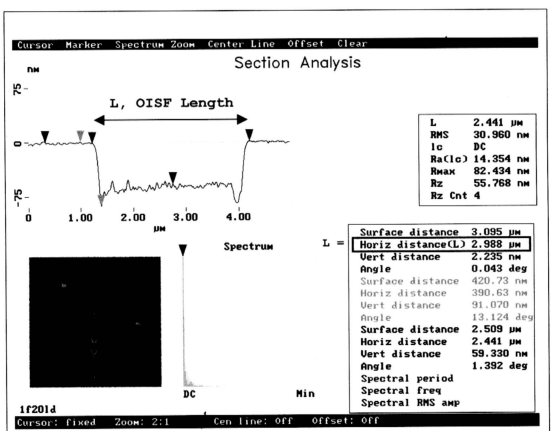

Figure 5.3 : OISF length measurement using AFM.

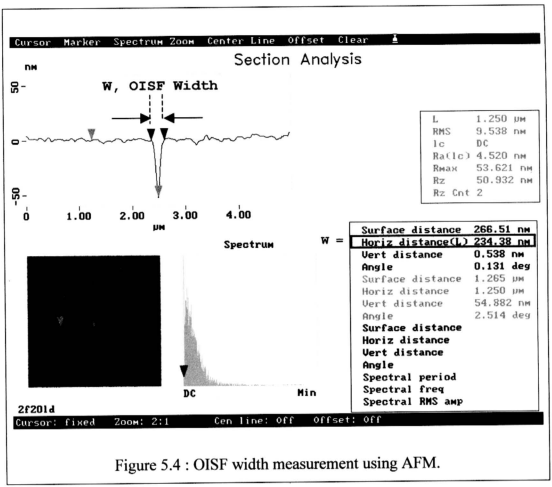

Figure 5.4 : OISF width measurement using AFM.

To overcome depth measurement problem by AFM, angular polishing technique was applied as alternative method to study OISF depth. (100) and (111) wafers were sand-blasted using different blasting pressure. This is followed by the standard heat treatment to induce the OISF formation and HF dipping.

HF dipped wafer was cleaved along wafer's natural cleaving planes into smaller pieces. Cleave pieces were angular-polished (*Refer Figure 5.5 and Figure 5.6*), and etched preferentially. OISF depth was measured under optical microscope at 200 times magnification while OISF density is determined for each condition prepared by counting OISF density on three spots on non-angular polished surface of cleaved wafer.

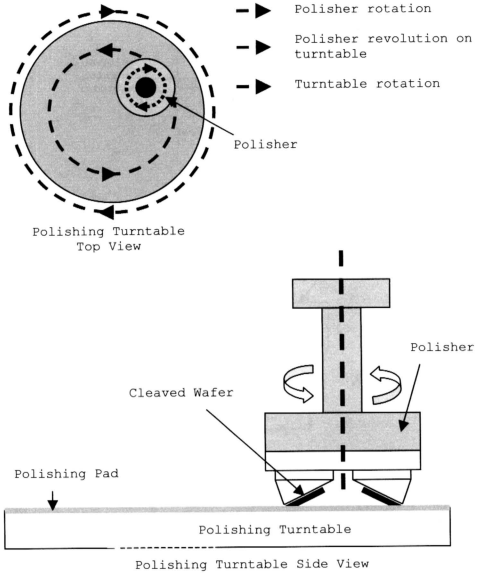

Figure 5.5 : Schematic diagram of angular polisher.

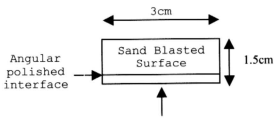

(a)

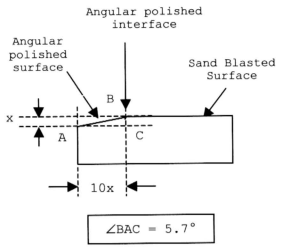

(b)

Figure 5.6 : (a) Top view and (b) side view of angular polished cleaved wafer

5.2.1 Results

5.2.1 OISF on (100) and (111) Wafers AFM Scanned Images

By using AFM and preferential etching technique, dimension of the same piece of OISF, at different surface removal, can be measured. For each 40μm x 40μm AFM scanned images there are about 15 to 30 pieces of OISFs. OISF length and width for the same piece of wafer at different surface removal was measured, and the average and standard deviation were calculated. From AFM scanned images obtained, OISFs formed on (111) wafer aligned 60° to one another while OISF formed on (100) wafer aligned 90° to one another.

As shown in Figure 5.7, there are four equivalent fault planes on (100) wafer where OISFs were formed. However there are only three equivalent fault planes on (111) wafer. Besides those differences mentioned, OISFs on (100) wafer also found to be longer compared to those formed on (111) wafer. AFM scanned images from (100) and (111) wafers at different surface removal were showed in Figure 5.8 and Figure 5.9 respectively. It was observed from the scanned images that OISF width increases with surface removal.

Figure 5.7 : Different OISF orientation found on (100) and (111) wafer

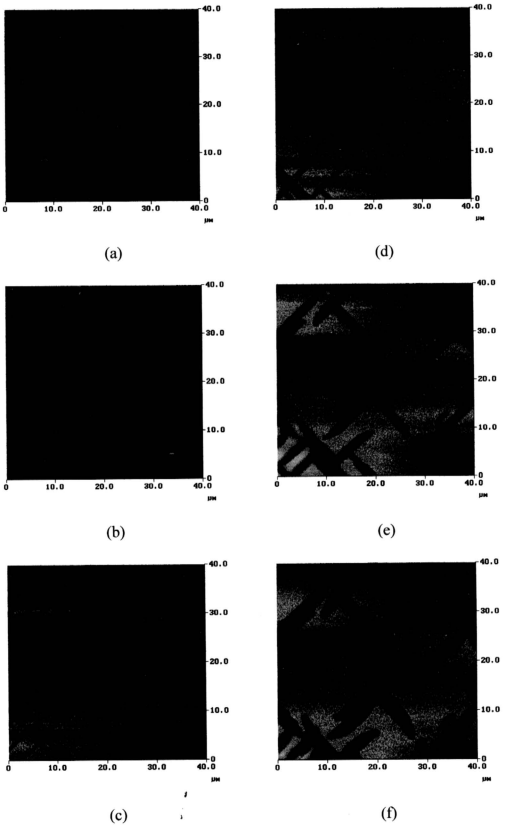

Figure 5.8 : (100) Wafer AFM scanned images after (a) 0.3μm, (b) 0.6μm, (c) 0.9μm, (d) 1.3μm, (e) 2.4μm and (f) 3.3μm surface removal.

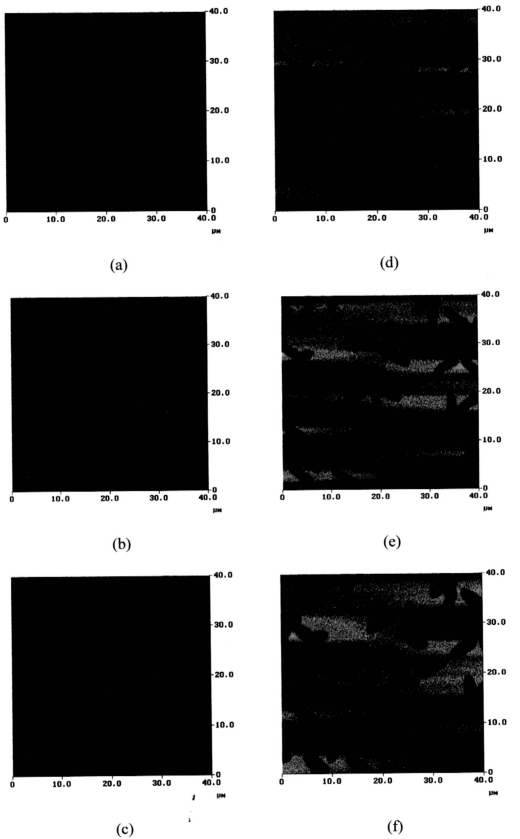

Figure 5.9 : (111) Wafer AFM scanned images after (a) 0.3μm, (b) 0.6μm, (c) 0.9μm, (d) 1.3μm, (e) 2.3μm and (f) 3.2μm surface removal.

In the wafer thickness measurement, direct measurement of polished (100) and (111) wafer is not practiced to avoid the dial gauge probe from damaging wafer surface during measurement. Besides 1μm resolution of the digital dial gauge used is incapable of detecting small change in wafer thickness by direct measurement. To overcome this problem, calculated thickness removal was used. The range of surface removal studied was 0.3μm to 3.5μm.

5.2.2 OISF Width as a Function of Surface Removal

OISF width of each individual OISF was measured from AFM images scanned at different surface removal. The average of OISF widths measured was found comparable between (100) and (111) wafers. When surface removal changed from 0.3μm to 3.3μm, the average of OISF width increased linearly from 0.3μm to 3.0μm regardless of wafer crystal orientation as shown in Figure 5.10.

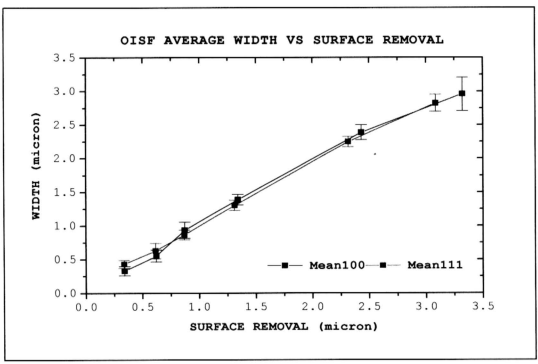

Figure 5.10 : OISF width at different surface removal for (100) and (111) wafers.

5.2.3 OISF Length as a Function of Surface Removal

OISF length was also obtained from those scanned images. OISF length plotted against surface removal is showed in Figure 5.11. OISF length change shown was compiled from about 40 pieces of OISF for each types of surface orientation. Instead of increasing linearly with surface removal, as observed in OISF width, OISF length showed very little change with surface removal. Besides, OISF length for (100) wafer is significantly longer than (111) wafer (*Refer Figure 5.12*).

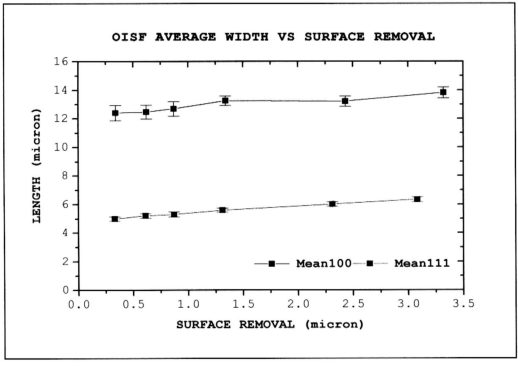

Figure 5.11 : OISF length at different surface removal for (100) and (111) wafers

OISF length for (100) and (111) wafers are given by :

$$L_{(100)}\,(\mu m) = 0.0005 * \text{surface removal} + 12.3$$

$$L_{(111)}\,(\mu m) = 0.0005 * \text{surface removal} + 4.91$$

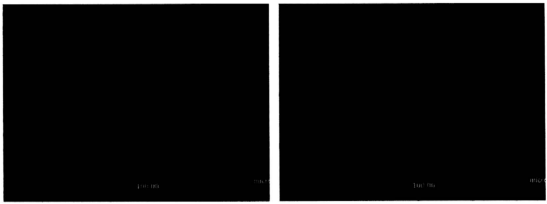

(100) Wafer (111) Wafer

Figure 5.12 : OISF formed on (100) and (111) wafers observed under 1000x magnification by optical microscope.

The slopes of both (100) and (111) wafers in Figure 5.11 are the same therefore the rates of change in OISF length for both (100) and (111) wafer as a function of surface removal are comparable. The OISF length changes slowly. For each micron of surface removal, there will an increase of OISF length of 0.0005μm. This value is so small that it is beyond the resolution of the dial gauge used. OISF length for (100) wafer is approximately 12.3μm while 5.0μm for (111) wafers. OISF with different length was always observed in (100) wafer but not in (111) wafers. The length uniformity in is much higher in OISFs from (111) wafer compared to those of (100) wafers.

5.2.4 OISF Depth as a Function of Blasting Pressure

Angular polishing technique exposed wafer regions from different depth from surface. When the angular polished wafer is etched using preferential etchant, OISF can be observed at different depth at angular polished region. Depth from wafer surface, the normal depth, which contains OISF is measured. Actual depth can be derived from normal depth when the inclined angle of OISF plane is known. (*Refer Figure 5.13 and Chapter 5.3*)

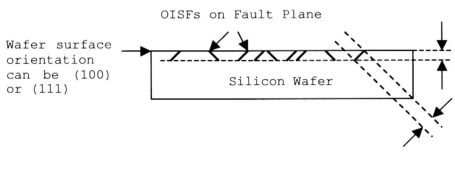

Actual Depth Calculation

$AD_{(100)} = ND_{(100)} / Sin\theta_{(100)}{}^{\circ}$

$AD_{(111)} = ND_{(111)} / Sin\theta_{(111)}{}^{\circ}$

θ is the inclined angle of fault plane with wafer surface

Figure 5.13 : Normal depth and actual depth measurement at wafer cross section.

Average of normal depth at different blasting pressure for both (100) and (111) wafers were as showed in Figure 5.14. Data from Figure 5.14 was calculated from the normal depth of 40 measurement points at angular-polished interface. The images of angular polished surface and interface of different blasting pressure

were shown in Figure 5.15. These images were captured by optical microscope at 200x magnification. The measured OISF normal depth was showed in these images.

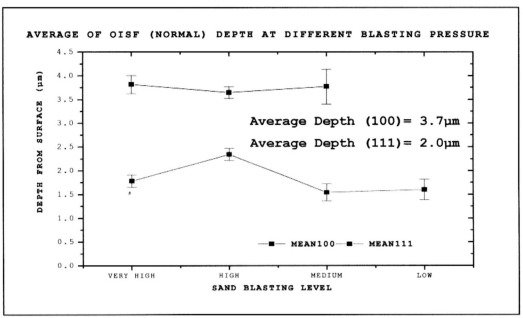

Figure 5.14 : OISF normal depth Vs blasting pressure (angular polishing technique).

OISF average normal depth for (100) wafer is 3.7µm while OISF normal depth is only 2.0µm for (111) wafer. For both (100) and (111) wafers, their normal depth does not change significantly with different blasting level, except for (111) wafer that showed slight increment in depth when wafer was blasted with high sand blasting condition.

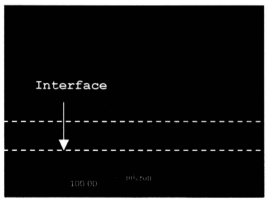

(a) (100), BP : Very high

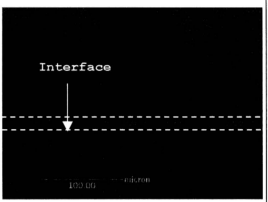

(d) (111), BP : Very high

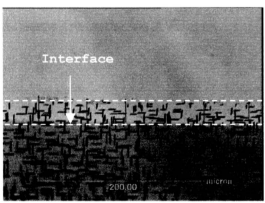

(b) (100), BP : High

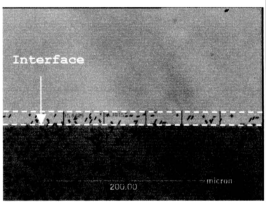

(e) (111), BP : High

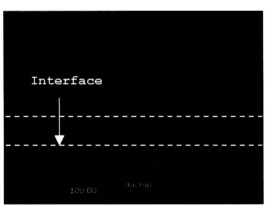

(c) (100), BP : Moderate

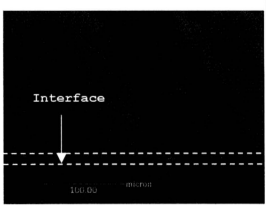

(f) (111), BP : Moderate

Figure 5.15 : OISF depth from angular polished surface. (a) to (c) for (100) wafer and (d) to (f) for (111) wafer. Magnification 200x. *Normal depth = (measured depth)/10 + surface removal by etching. BP = blasting pressure.*

5.3 Discussion

5.3.1 OISF Length and Width Comparison between (100) Wafer and (111) Wafer

For length and width measurement, an area of 40μm x 40μm on the wafer was scanned using a grid of 512 points by 512 points. Selected surface area was scanned point by point along a line. The line scanning will be restarted at the adjacent line in the same manner.

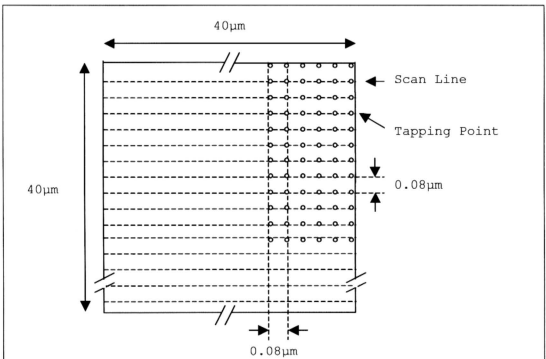

Figure 5.16 : Wafer surface scanning using AFM for scanned area of 40μm x 40μm.

There are 512 horizontal scan lines in the 1600μm^2 scanning area. For each scan line, there are 512 tapping points. As illustrated in Figure 5.16, the point-to-point separations and the distances between the lines are equal to 0.08μm when grid and scanned area mentioned above is used. This separation calculated represents the resolution for OISF length and width measured using AFM.

According to measured OISF length and width, the typical OISF length for (100) and (111) wafers are 5μm and 12μm respectively. In terms of OISF width measured, both types of wafers have OISF width ranged from 0.3μm to 0.4μm after 20 seconds preferential etching. Since resolution of 0.08μm obtained is much higher compared to width and length measured therefore OISF length and width measured represents the actual length and width of OISFs within the area scanned.

OISF length is determined by OISF growth. The growth of OISF depends on many factors such as oxidation time, oxidation ambient, crystal orientation, and dopant concentration. The length of OISF, L, oxidized in 100% oxygen at various temperatures is given by [4, 10]

$$L(\mu m) = A\, t^{n} \exp(-Q/kT)$$

A, Q, t, n, k, and T are the constant, the activation energy of OISF growth, oxidation time, number exponent, Boltzmann constant and absolute temperature respectively.

Number exponent, n, is 0.8 while activation energy, Q, is 2.3eV, regardless of oxidation ambient and crystal orientation of substrates. Constant A [2, 4] for (100) and (111) wafers with different oxidation ambient is given in Table 5.1.

Table 5.1 : Values of OISF Growth Constant A in $L = A t^n \exp(-Q/kT)$ for Silicon [after Hu].

Orientation	**OISF Growth Constant, A**	
	Dry O_2 oxidation	**Wet O_2 oxidation**
(100)	2.28×10^9	4.16×10^9
(111)	1.09×10^9	1.53×10^9

A comparison between calculated length and measured length in the experiment is given in Table 5.2. Calculated lengths for (100) and (111) wafers are 15.45μm and 5.68μm respectively. Measured length lies in the same order of magnitude with calculated length. Measured OISF length for (111) wafer is 12~13μm while the measured OISF length for (100) wafer is 5~6μm.

Table 5.2 : Comparing OISF Length : Calculated Value Vs Experimental Value.

Description	**Unit**	**(100)**	**(111)**
A, constant	-	4.16×10^9	1.53×10^9
t, oxidation time	hr	1	1
n, number exponent	-	0.8	0.8
Q, activation energy	eV	2.3	2.3
k, Boltzmann constant	eV/°K	8.63×10^{-5}	8.63×10^{-5}
T, oxidation temperature	°K	1373	1373
L_C, Calculated Length $= A t^n \exp(-Q/kT)$	**μm**	**15.45**	**5.68**
L_M, Measured Length	**μm**	**12~13**	**5~6**

OISF length and width at any surface removal studied is uniform. This characteristic is typical for OISF formed on mechanically damaged surface [7, 20, 21, 23]. Uniformity in OISF dimension is associated with heterogeneous nucleation [4, 10, 23], common OISF origin [3] and their simultaneous formation

[10]. In heterogeneous nucleation, OISF will be nucleated at dislocation or defects simultaneously. The occasionally observed variation in the size of bulk OISF is attributed to a continuous formation of stacking fault nucleus [4].

Consistent with Hu's finding [4], OISF length for (100) wafer was 2.4 times that of (111) wafer's OISF length. Hu found that OISF formed on (100) wafer is about two times of those on (111) wafer [5]. The difference in OISF length on difference crystal orientation may influence metallic gettering efficiency of sand blasted wafer.

Cu is one of the very volatile elements in silicon wafer even at room temperature. The device performance will be deteriorated with the presence of Cu in silicon wafer. Cu diffusion into a mechanically polished silicon wafer is temperature dependent [23]. At 1000°C or less, precipitation takes place along dislocation lines. Since OISF formed on (100) wafer is much longer than (111) wafer, there may be more sites for Cu precipitation during gettering.

If the amount of Cu that can be precipitated depends on the length of dislocation line, then gettering efficiency will depend on OISF length. Similarly when OISF density of (100) and (111) wafers are the same, due to its longer OISF, the former may have higher gettering efficiency compared to the latter, when they are subjected to the same Cu precipitation condition.

(100) wafer and (111) wafer having same OISF density are shown in Figure 5.17. In this figure, circles with diameter of OISF length were drawn enclosing one OISF each. Cu precipitation is believed to happen within the circles drawn.

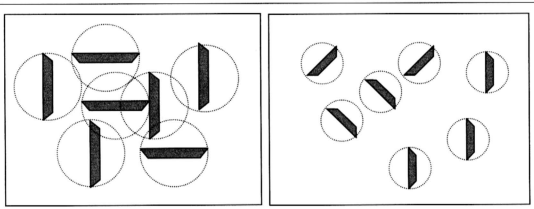

(100) (111)

Figure 5.17 : Radius of effective gettering for (100) and (111) wafer having same OISF density.

The area enclosed by the circle is presumed to be the locus of effective metal precipitation at OISF because the presence of higher stress at dislocation points. Therefore Cu precipitation is more likely to happen within the overlapped region of the circles that is considered as highly stressed region. When Cu precipitation efficiency of (100) and (111) wafers having same OISF density were compared, (100) wafer may be more efficient compared to (111) wafers due to its longer length.

OISF width measured at different surface removal for (100) and (111) wafers were comparable regardless of surface removal. When (100) and (111) wafer's OISFs were delineated, further wafer etching will remove silicon atoms layer by

layer from the surface. At the same time, OISF width widening was observed in further etching (Refer Figure 5.18).

Etching rate of silicon wafer is dependent of crystal orientation. OISF for both (100) and (111) wafers were formed on the same {111} fault planes (*Explanation is given in Chapter 5.3.2*) therefore the OISF inner walls for (100) and (111) wafers would experience the same etching rate.

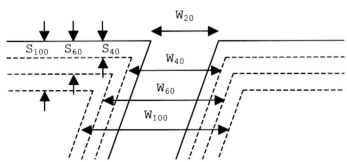

OISF Width, W_{time}		Surface Removal, S_{time}	
W_{20}	= after 20s etching	S_{40}	= after 40s etching
W_{40}	= after 40s etching	S_{60}	= after 60s etching
W_{60}	= after 60s etching	S_{100}	= after 100s etching
W_{100}	= after 100s etching		

Figure 5.18 : OISF width measured at different surface removal.

OISF fault planes were inclined at different angle to (100) and (111) wafers surface. The little difference in inclined angles will not impact the width measured substantially hence the OISF width as a function of surface removal exhibited in Figure 5.10 are the same regardless of crystal orientation (*Refer Appendix C*).

5.3.2 OISF Fault Plane Identification for (100) and (111) Wafer

Compared to width and length determined, depth measurement by AFM is affected by the geometry of OISF as well as silicon tip used. It is inevitable that silicon tips etched from the same piece of wafer would have different etched geometry. To enable further study of OISF formed on (100) and (111) wafers, the actual fault planes of both types of wafers were confirmed using cleaved-etch technique.

Sand blasted (100) and (111) wafers were oxidized to generate OISF. After oxide layer removal, wafers were cleaved along its cleave planes followed by preferential etching. Figure 5.19 showed cleaved planes for both surface orientations while Figure 5.20 displayed the micrographs of (100) and (111) wafer captured using SEM at the cleaved surface.

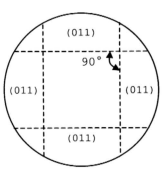

(100) Wafer

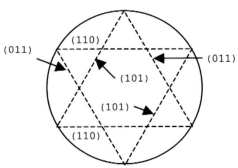

(111) Wafer

Figure 5.19 : Cleave planes for (100) and (111) wafers.

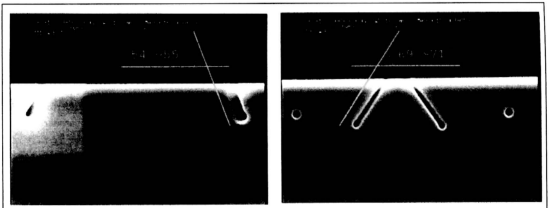

(100) wafer (111) wafer

Figure 5.20 : SEM micrograph at cleaved surface for (100) and (111) wafers.

Angle between wafer surface and fault plane was measured on SEM micrographs in Figure 5.20. On (111) wafer surface, the faults lie at angle of ~70° to surface while on (100) wafer surface, the fault plane is inclined at ~55° to the surface. A table of possible fault planes, $\{h_2k_2l_2\}$, for (100), (110) and (111) surface plane, $\{h_1k_1l_1\}$, is shown in Table 5.3.

Table 5.3 : Inter-planar Angles between Surface Planes $\{h_1k_1l_1\}$ and Fault Planes $\{h_2k_2l_2\}$ in Silicon (Cubic) [2].

Surface Plane,	**Fault Plane, $\{h_2k_2l_2\}$**		
$\{h_1k_1l_1\}$	**100**	**110**	**111**
100	2 of 90.00°	4 of 45.00° 2 of 90.00°	**4 of 54.74°**
110	4 of 45.00° 2 of 90.00°	4 of 60.00° 1 of 90.00°	2 of 35.26° 2 of 90.00°
111	3 of 54.74°	3 of 35.26° 3 of 90.00°	**3 of 70.53°**

All OISF regardless of whether they are observed on (100) or (111) surface, lie along {111} planes. OISF on (111) wafer lies along three {111} planes while OISF on (100) wafers lie along four {111} planes. Surface damage present on the entire surface of sand blasted wafer causes this surface to be highly stressed. During wafer oxidation, stress at damaged sites (atom displacements) is released by plane slippage process resulted in OISF formation.

Plane slippage normally happens to planes with highest packing density therefore OISF formed on {111} planes regardless of surface crystal orientation of wafer used. When surface orientations of wafer are different but their fault plane are the same, difference in OISF feature between (100) and (111) was observed.

5.3.3 Limitation of OISF Depth Measurement Using AFM

OISF depth cannot be measured using AFM tapping mode. The measurement limitation by the tip and OISF geometry is explained in this portion of the dissertation. For any scanning in the direction parallel to the cantilever using silicon tip with realistic shape (*Refer Figure 3.5*), any wall angle on the left wall that is more than 55° will be shown as 55° in the image. Any wall angle on the right wall that is more than 70° to 80° will be shown as 70° to 80° in the image.

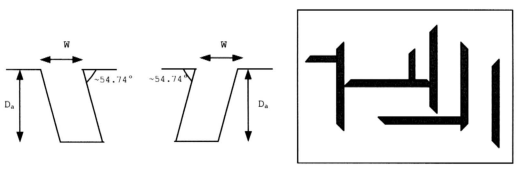

(100) Wafer

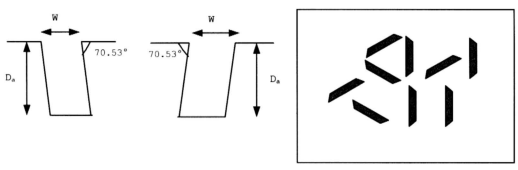

(111) Wafer

Figure 5.21 : Illustration of cross sectional view for OISF orthogonal to scanning direction from (100) and (111) wafers.

Figure 5.21 illustrates the cross section of OISF from different crystal orientation and its inclined angle. When cantilever where silicon tip is mounted is not tilted, the length of silicon probe tip is 12μm while its width is 8μm. Silicon tip length is much longer than the depth of OISF delineated. Measurable depth by the probe tip is therefore limited by the width of OISF formed while depth profile of OISF measured is limited by the shape of silicon probe tip and inclined angle between (111) plane and surface.

If fault plane for (100) wafer is slanted to the left (*Refer Figure 5.22(a)*), either a near symmetrical valley or a near symmetrical flat-base valley depth profile will be obtained. The profile of OISF, obtained from AFM, is determined by the relative depth between of OISF and D_{m1}.

Figure 5.22(b) shows (100) wafer having (111) plane slanted to the right with θ_1 ~55°. Silicon tip used able to measure the slope angle of the left wall nearest to the truth due to the slope angle of the wall is also ~55°. The inclined behavior of the fault plane causes the right wall of OISF cannot be measured correctly. The right wall profile will be measured as a slope having an angle of 70°~80° which is not the actual profile of OISF depth.

If the OISF actual depth is D_1, then depth measured, D_{m1}, in Figure 5.22(b), indicated by the blue dotted line is less than the actual depth. In this case, depth profile obtained will be a non-symmetric valley. If actual depth is D_2, then the measured depth, D_{m2}, indicated by the red dashed line, is the true depth. Depth profile will look like a non-symmetric flat-based valley.

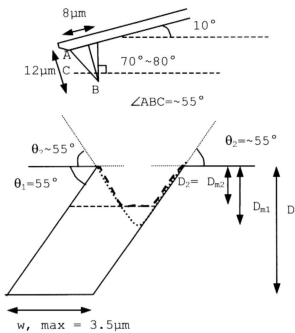

(a)

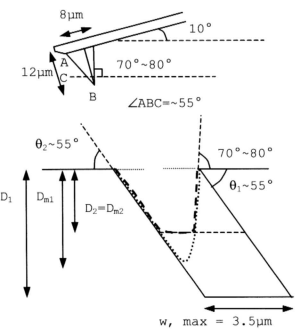

(b)

Figure 5.22 : Simulation of AFM tapping mode OISF depth measurement on (100) wafer having OISF fault plane (a) slanted to the right with θ_1~55°, (b) slanted to the left with θ_1 ~55°.

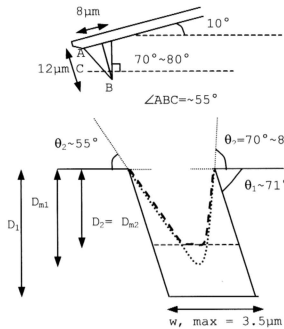

(a)

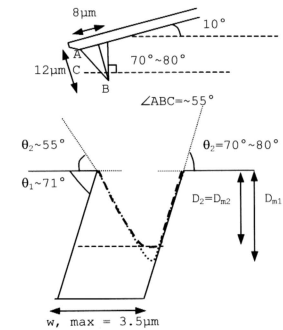

(b)

Figure 5.23 : Simulation of AFM tapping mode measurement on (111) wafer having OISF fault plane (a) slant to the right with θ_1 >55°, (b) slant to the left with θ_1 >55.

The inclined angle between (111) surface plane and (111) fault planes is ~71°. Similarly, if OISF lying on the fault plane is slanted to the right, left wall slope measured was around 55° due to the shape of silicon probe tip used. Angle on the right wall is more than 70° to 80°, therefore right wall will be slanted at only 70° to 80°, as shown in Figure 5.23(a). Profile obtained is non-symmetric.

When fault plane is slanted to the left, the same profile with the right side slanted fault plane profile will be obtained. This is due to the left wall angle is much greater than 55° (the tip's right slope) and the left wall slope angle of this OISF is about the same as the left angle of the silicon probe tip. If the actual depth of OISF is greater or equal to D_{m1}, a non-symmetrical valley will be obtained. If the true depth is shallower than D_{m1}, for example D_2, then a flat-base non-symmetric valley will be observed in the cross sectional graph.

If the depth profile obtained from AFM measurement has a flat base characteristic, depth measured, if not the true depth, will be very near the actual depth. In the case where valley depth profile obtained was non-flat base, we cannot conclude that the measured depth is the true depth. The depth measured is highly possible not the true depth of OISF, and the depth profile obtained is definitely untrue. This is applicable for both crystal orientations studied. Therefore OISF depth measurement using AFM is not accurate and depth profile obtained would be misleading.